

CASCADING OF FAST-MODE BALANCED AND IMBALANCED TURBULENCE

T. K. SUZUKI¹, A. LAZARIAN², A. BERESNYAK²

Submitted to ApJ

ABSTRACT

We study the cascading of fast MHD modes in magnetically dominated plasma by performing one-dimensional (1D) dynamical simulations. We find that the cascading becomes more efficient as an angle between wave vector and underlying magnetic field increases and fast mode becomes more compressive. We also study imbalanced turbulence, in which wave packets propagating in one-direction have more power than those in the opposite direction. Unlike imbalanced Alfvénic turbulence, the imbalanced fast mode turbulence shows faster cascading as the degree of imbalance increases. We find that the spectral index of the velocity and magnetic field, which are carried by the fast-mode turbulence, quickly reaches stationary value of -2 . Thus we conclude that the dissipation of fast mode, at least in 1D case, happens not due to weak or strong turbulent cascading, but mostly due to nonlinear steepening. The density fluctuations, which are carried by slow-mode perturbation in the larger scale and entropy-mode perturbation in the smaller scale, depend on initial driving spectrum and a ratio of specific heat.

Subject headings: magnetohydrodynamics – plasma – turbulence

1. INTRODUCTION

Magnetohydrodynamical (MHD) turbulence is ubiquitous in astrophysics. All interstellar medium (ISM) phases are well magnetized with Larmor radius of thermal proton much smaller than outer scale. Molecular clouds are no exception, with compressible, often high-Mach number, magnetic turbulence determining most of their properties (see Elmegreen & Falgarone 1996, Stutzki 2001). Star formation (see McKee & Tan 2002; Elmegreen 2002; Pudritz 2002; Ballesteros-Paredes et al. 2006), cloud chemistry (see Falgarone 1999 and references therein), shattering and coagulation of dust (see Lazarian & Yan 2002 and references therein) are examples of processes for which knowledge of turbulence is absolutely essential. It is also believed that MHD waves and turbulence are important for the acceleration of the solar wind (e.g. Tu & Marsch 1995) as well as winds from stars which possess surface convective layers (e.g. Tsuji 1988).

As MHD turbulence is an extremely complex process, all theoretical constructions should be tested thoroughly. Until very recently matching of observations with theoretical constructions used to be the only way of testing. Indeed, it is very dangerous to do MHD turbulence testing without fully 3D MHD simulations with a distinct inertial range. Theoretical advances related to the anisotropy of MHD turbulence and its scalings (see Shebalin et al. 1983, Higdon 1984, Montgomery, Brawn & Matthaeus 1987, Shebalin & Montgomery 1988, Zank & Matthaeus 1992) were mostly done in relation with the observations of fluctuations in solar wind. Computers allowed an important alternative way of dealing with the problem. While still presenting a limited inertial range,

they allow to control the input parameters making it easier to test theoretical ideas.

It is well known that linear MHD perturbations can be decomposed into Alfvénic, slow, fast, and entropy modes with well-defined dispersion relations (see Alfvén & Fälthammar 1963). The separation into Alfvén and pseudo-Alfvén modes, which are the incompressible limit of Alfvén and slow MHD modes, is an essential element of the Goldreich-Sridhar (1995, henceforth GS95) model of turbulence. There the arguments were provided in favor of Alfvén modes developing a cascade on their own, while the pseudo-Alfvén modes being passively advected by the cascade. The drain of Alfvénic mode energy to pseudo-Alfvén modes was shown to be marginal.

The separation of MHD perturbations into modes in compressible media was discussed further in Lithwick & Goldreich (2001) and Cho & Lazarian (2002, 2003 henceforth CL02, CL03, respectively). Even though MHD turbulence is a highly non-linear phenomenon, the modes does not constitute an entangled inseparable mess.

The actual decomposition of MHD turbulence into each mode was a challenge that was addressed in CL02, CL03. They studied a particular realization of turbulence with mean magnetic field comparable to the fluctuating magnetic field. This setting is, on one hand, rather typical of the most MHD flows in Galaxy and, on the other hand, allows them to use a statistical procedure of decomposition in the Fourier space, where the bases of the Alfvén, slow, fast, and entropy perturbations were defined. The entirely different way to decompose modes in high or low- β cases in real space was shown in CL03 to correspond well to this procedure³.

In particular, calculations in CL03 demonstrated that fast modes are marginally affected by Alfvén modes and follow acoustic cascade in both high and low β medium. In Yan & Lazarian (2002; 2004; henceforth YL04) the fast modes were identified as the major agent in scatter-

³ In CL03, an isothermal equation of state is used so that entropy-mode fluctuation is prohibited.

Electronic address: stakeru@ea.c.u-tokyo.ac.jp

Electronic address: lazarian, andrey@astro.wisc.edu

¹ School of Arts and Sciences, University of Tokyo, 3-8-1, Komaba, Meguro, Tokyo, 153-8902, Japan

² Department of Astronomy, University of Wisconsin, 475 N. Charter St., Madison, WI 53706

ing of cosmic rays. Similar results in relation to stochastic acceleration of cosmic rays were reached in Cho & Lazarian (2006). Interestingly enough, the dominance of fast modes for both acceleration and scattering is present in spite of the dissipative character of fast modes. The reason for that is isotropy⁴ of this mode reported in CL03. The Alfvén modes, that are still the default for scattering and acceleration for many researchers, are inefficient due to the elongation of eddies along the magnetic field (Chandran 2000, Yan & Lazarian 2002).

Apart from cosmic rays, acceleration of charged interstellar dust is also dominated by fast modes (Lazarian & Yan 2002, Yan & Lazarian 2003). In stellar magnetospheres with spiral magnetic fields, fast-modes possibly play a role in energetics and dynamics of winds from usual stars (Suzuki et al. 2006) and pulsars (Lyubarsky 2003). These issues provide an additional motivation to studies of properties of fast mode cascade.

The most efficient interaction of fast modes is expected to happen for waves moving in the same direction (see CL02). This indicates that, unlike studies of Alfvén modes for which the 3D character of interactions is essential, 1D simulations could still give, at least in some respects, correct physical properties of the fast-mode turbulence. 1D simulations have a big advantage that we can use a number of grid points for a broader inertial range than 2D or 3D simulations. Based on these issues, we carry out 1D decay simulations of fast-mode turbulences. We should cautiously analyze simulation data, because the 1D geometry systematically enhances shocks without dilution to the tangential directions.

In what follows we discuss our code in §2, calculate power spectra in §3, and study cascading of fast modes in §4. We discuss our findings in §5.

2. THE CODE AND THE SIMULATIONS SETUP

We initially give perturbations of fast mode by fluctuations of longitudinal velocity, v_x , transverse velocity, v_y , transverse magnetic field, B_y , density, ρ , and pressure p (or specific energy, $e = \frac{p}{(\gamma-1)\rho}$, where γ is a ratio of specific heat) in magnetically dominated plasma, namely low- β conditions. We dynamically treat time evolution of each variables by solving ideal MHD equations without continuous driving (decay simulation). We do not consider the third (z) component of magnetic field and velocity, which indicates that Alfvén mode is switched off in our simulation, whereas fast, slow, and entropy modes are automatically treated. We assume one-dimensional approximation, namely all the physical variables depend only on x ; a wave number vector has only the x -component, namely, $k = k_x$. The number of grid points of the x component is $65536 (= 2^{16})$, and the periodic boundary condition is imposed in x -direction.

⁴ Recent calculations of fast modes interacting with Alfvén modes by Chandran (2005) indicate some anisotropy of fast modes. In particular, he shows that contours of isocorrelation for fast modes get oblate with shorter direction along the magnetic field. However, the calculations are performed assuming that Alfvén modes are in the weak turbulence regime. This regime has a limited inertial range. Moreover, anisotropic damping discussed in YL04 is probably a more strong source of anisotropy. Anyhow, the above conclusions about the dominance of fast modes are not altered by the anisotropies that corresponds to squashing contours of isocorrelations in the direction of magnetic field.

$$\frac{d\rho}{dt} + \rho \frac{\partial v_x}{\partial x} = 0, \quad (1)$$

$$\rho \frac{dv_x}{dt} = -\frac{\partial p}{\partial x} - \frac{1}{8\pi} \frac{\partial}{\partial x} (B_y^2) \quad (2)$$

$$\rho \frac{d}{dt} (v_y) = \frac{B_x}{4\pi} \frac{\partial B_y}{\partial x}. \quad (3)$$

$$\rho \frac{d}{dt} \left(e + \frac{v^2}{2} + \frac{B^2}{8\pi\rho} \right) + \frac{\partial}{\partial x} \left[\left(p + \frac{B^2}{8\pi} \right) v_x - \frac{B_x}{4\pi} (\mathbf{B} \cdot \mathbf{v}) \right] = 0, \quad (4)$$

$$\frac{\partial B_y}{\partial t} = \frac{\partial}{\partial x} [(v_y B_x - v_x B_y)], \quad (5)$$

where $B^2 = B_x^2 + B_y^2$ and $v^2 = v_x^2 + v_y^2$; $\frac{d}{dt}$ and $\frac{\partial}{\partial t}$ denote Lagrangian and Eulerian time derivatives.

The minimum wave number corresponds to the box size. We set-up $p = 1$, $\rho = 1$, $v_x = 0$, $v_y = 0$ as background conditions. We test two cases of the background magnetic fields, $(B_x, B_y) = (9, 3)$ (quasi-parallel) and $(B_x, B_y) = (3, 9)$ (quasi-perpendicular), and three cases of a ratio of specific heat, $\gamma = 5/3$ (adiabatic), 1.1 (nearly isothermal), and 1 (isothermal).

For the simulations we employed 2nd order nonlinear MHD Godunov-MOCCT scheme developed by Sano & Inutsuka (2007, in preparation) (see also Suzuki & Inutsuka 2005; 2006). In this scheme, each cell boundary is treated as discontinuity, for the time evolution we solve nonlinear Riemann shock tube problems with magnetic pressure by the Rankine-Hugoniot relations. Therefore, entropy generation, namely heating, is automatically calculated from the shock jump condition. A great advantage of our code is that no artificial viscosity is required even for strong MHD shocks; numerical diffusion is suppressed to the minimum level for adopted numerical resolution.

3. TIME EVOLUTION AND POWER SPECTRA

We firstly study time-evolution of the simulated turbulences and their power spectra. In this section, we present the results of quasi-parallel ($(B_x, B_y) = (9, 3)$) and $\gamma = 1.1$ case. The initial amplitude is set to be $dB_y = 4.4$, corresponding to super-sonic and sub-Alfvénic condition. Fast modes traveling in both directions have equal energies, we call this balanced turbulence. We test two types of initial spectral slopes; one is $\propto k^{-3/2}$ with random δ -correlated phases for all wavenumbers, and the other is $\propto k^0$, namely white noise. Note that $k^{-3/2}$ is a prediction of weak acoustic turbulence, which is supposed to have similar properties to weak fast-mode turbulence (CL02; CL03), whereas the validity of weak turbulence approximation is still under debate for acoustic turbulence (Falkovich & Meyer 1996; Zakharov, L'vov, & Falkovich 1992). Figures 1 & 2 present time-evolution of the cases with initial spectra $\propto k^{-3/2}$ and k^0 , respectively; the six panels present v_x , v_y , B_y , ρ , e , and p at $t = 0.5$ (dashed) and $t = 3.0$ (solid).

We also show the power spectra of v , B , and ρ at $t = 3.0$ in Figures 3 and 4. Although our initial conditions contain only fast mode, slow mode is generated by nonlinear process of mode interaction. In order to understand the interplay of modes, we decompose all values into fast and slow perturbations (see CL02). This

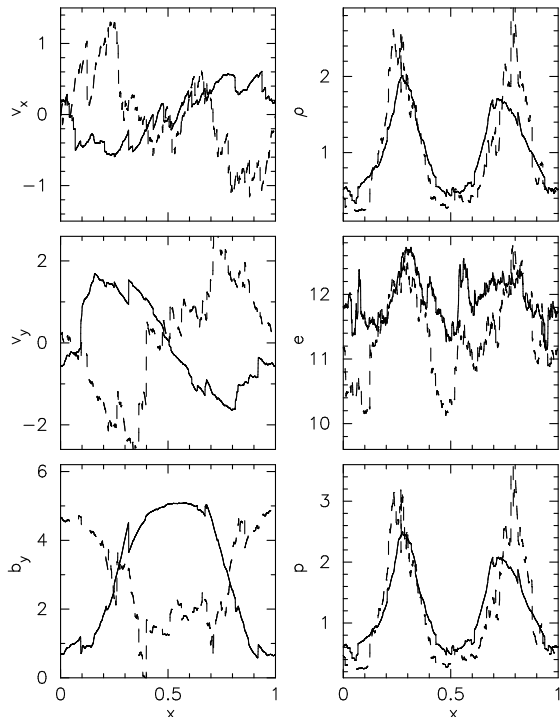


FIG. 1.— Evolution of v_x (top-left), v_y (middle-left), B_y (bottom-left), ρ (top-right), e (middle-right), and p (bottom-right). Dashed and solid lines are the results at $t = 0.5$ and $t = 3$, respectively. The initial spectral slope is $\propto k^{-3/2}$.

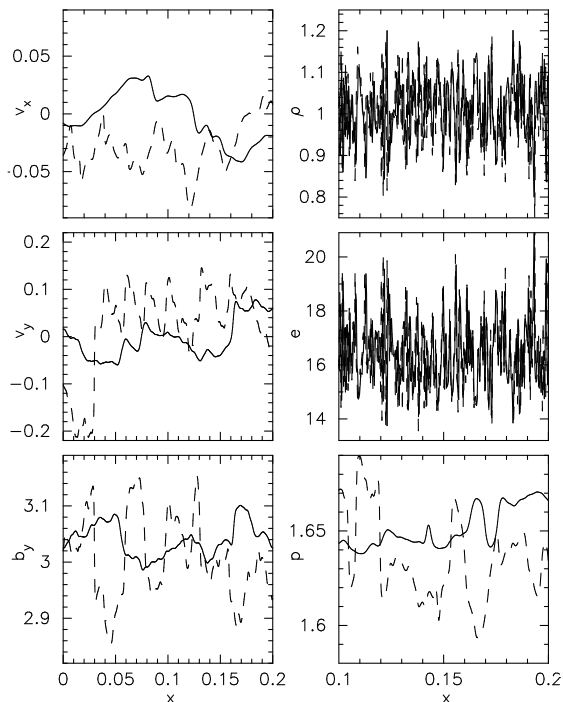


FIG. 2.— The same as Figure 1 but for white noise as the initial perturbation. Note that the horizontal axis is enlarged compared with Figure 1; the horizontal axis of the right panels is from $x = 0.1$ to 0.2 , while that of the left panels is from $x = 0$ to 0.2 .

method is statistically correct even for nonlinear waves as discussed in CL03. In Figures 3 and 4, the decomposed spectra of fast (left) and slow (middle) modes as well as the raw spectra (right). Note that the B_y and ρ spectra of the slow mode in the initial white noise case (Figure 4) may contain errors in the small scale (large k) region. As we describe later, the density perturbation is mainly due to entropy-mode in this case. The slow mode spectrum is calculated from the subtraction of the dominated entropy mode from the total power, which might leave an error in the slow mode. The B_y spectrum of the slow mode, which is connected to the slow mode density spectrum through the frozen-in condition, might also contain non-negligible errors.

The velocities and magnetic fields exhibit many discontinuities, i.e. fast and slow MHD shocks, in both cases (the left panels of Figures 1 & 2). The amplitudes of the white noise case is much smaller than those of the $k^{-3/2}$ spectrum case, because the white noise perturbations initially contain more energy in smaller scales which suffer faster damping.

Figures 3 & 4 indicates that the velocity and magnetic field perturbations are carried by fast mode. This is first because the slow mode is downconverted from the fast mode, and second because the fast wave becomes magnetic mode in low- β medium. The slow wave essentially corresponds to hydrodynamic (acoustic) mode, and this is the main reason why the slow-mode perturbation dominates the fast-mode in the density spectra, in accordance with the earlier claims in CL03, Passot & Vázquez-Semadeni (2003), and Beresnyak et al. (2005), whereas the entropy-mode perturbation is also important in the initial white noise case as discussed later.

As expected from many discontinuities in Figures 1 & 2, v and B_y exhibit shock dominated spectra, $\propto k^{-2}$ in both $k^{-3/2}$ (Figure 3) and white noise (Figure 4) cases. This indicates that the weak cascade solution of acoustic turbulence ($\propto k^{-3/2}$) does not hold for any significant time even though it is provided initially. The randomness of phases typically assumed in acoustic turbulence or in other theories of weak turbulence breaks down quickly by nonlinear interaction, leading to Burgers-like shock-dominated random state. This is different from the results of the 3D simulation by CL02 in which spectrum $k^{-3/2}$ is suggested. The difference may be due to the difference of 1D vs. 3D cases; the effect of shocks tend to become systematically predominant in 1D simulations because shocks do not dilute geometrically.

Since our simulations do not assume isothermal gas, the different dissipation characters influence the evolution of thermal properties. The initial specific energy, $e_0 (= \frac{p_0}{(\gamma-1)\rho_0})$, is 10 in both cases. In the $k^{-3/2}$ case, the heating is localized at first in places where strong shock heating takes place; at $t = 0.5$, e partially becomes $\gtrsim 12$, while some places stay $e \approx e_0 (= 10)$. Most places experience the heating eventually and at $t = 3.0$ the gas is averagely heated up to $e \approx 12$. On the other hand, in the white noise case (Figure 2), e is quickly heated to $e \approx 17$ because of the rapid dissipation, and after that e stays almost constant with time.

The densities show different features in Figures 1 and 2; the ρ structure of the initial $k^{-3/2}$ spectrum case (Figure 1) is dominated by larger scale with a couple of shocks,

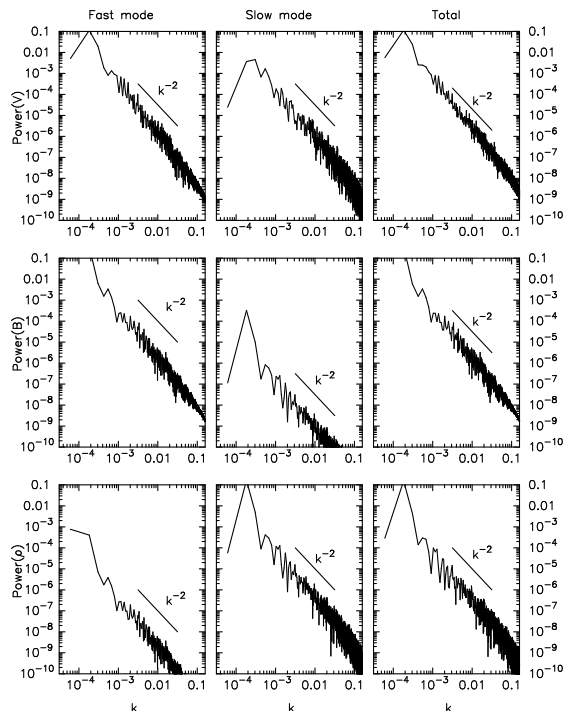


FIG. 3.— Power spectra of v (top), B (middle), and ρ (bottom) decomposed into fast (left) and slow (middle) modes at $t = 3.0$ for the initial $\propto k^{-3/2}$ perturbation. Composed values are shown on the right for comparison.

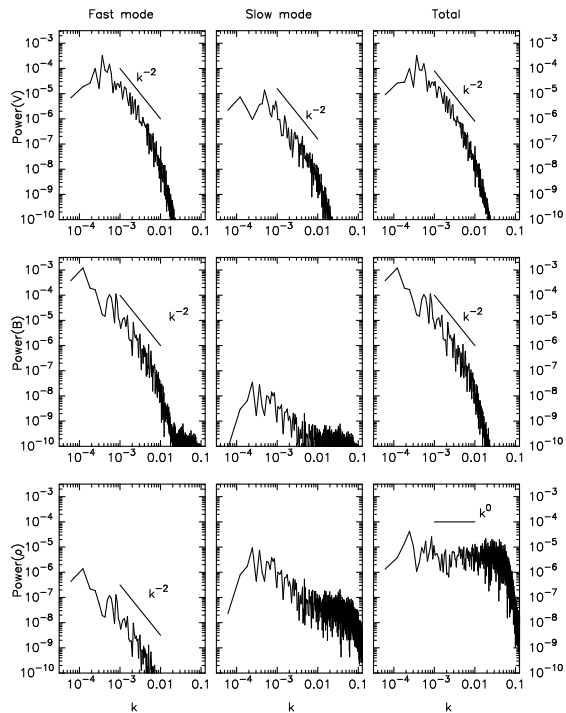


FIG. 4.— Same as Figure 3 but for the initial white noise perturbation. Note that the composed density spectrum is mainly owing to entropy mode (note show); this is the reason why the total power of the density turbulence is larger than the combination of the fast- and slow-mode perturbations. The slow mode B_y and ρ spectra might contain errors in the high k region (see text).

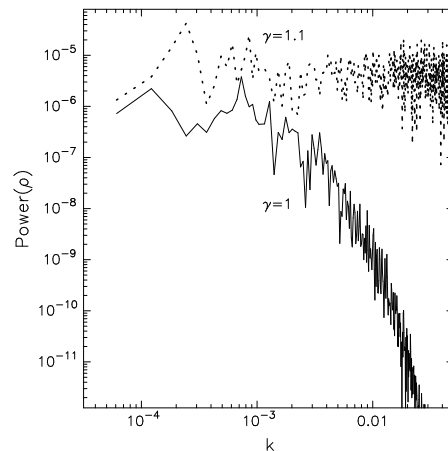


FIG. 5.— Density spectra of the initial white noise perturbations for $\gamma = 1.1$ (dotted) and 1 (dashed) at $t = 3$.

which is qualitatively similar to v and B_y , while many small-scale structures are predominant in the white noise case (Figure 2). Figure 3 ($k^{-3/2}$ case) shows the density perturbation is mainly carried by the slow-mode and the spectral slope is the shock-dominated one, k^{-2} , similarly to the B_y and v spectra.

On the other hand, in the initial white noise case, the total power of the density fluctuation (the right bottom panel of Figure 4) is much larger than the sum of the fast- and slow-mode perturbations. In fact, the density perturbation in this case is mostly owing to an entropy mode, which is a zero-frequency mode with unperturbed p and with perturbed ρ and e (see e.g. Lithwick & Goldreich 2001). By a close look at Figure 2 one can see that the phases of e and ρ , both of which show small-scale structure, are anti-correlated so that $p(\propto \rho e)$ shows a smooth feature. The initial perturbations (white noise) contain sizable energy in the small scale. These small-scale turbulences quickly dissipate, rather than converted to slow-mode perturbation, to entropy-mode fluctuation. The density fluctuation of the entropy mode drives the fluctuation of the energy deposition by shocks. The heating rate per unit mass is larger in hotter regions because of the lower density, which self-sustains the entropy-mode perturbation. As a result, the density perturbation is preserved with keeping the initial flat spectrum until the end of simulation ($t = 3$), when the turbulent energy of the fast mode decays $\simeq 1/1000$ of the initial value.

In conclusion, the density perturbation is controlled by initial driving turbulence (see Beresnyak 2005 for 3D case). This is a kind of bistability. When the energy is given in a larger scale, the density perturbation is carried by the slow-mode downconverted from the fast-mode. The generated slow-mode shows the shock-dominated spectrum. On the other hand, when the energy is input in a smaller scale, the density perturbation is self-sustained by the entropy-mode fluctuation, which is a result of the dissipation of the fast-mode turbulence. The density perturbation triggers the fluctuation of the heating, which sustains the entropy-mode fluctuation in itself. In this case, an initial spectrum is preserved in the density perturbation.

In isothermal ($\gamma = 1$) gas, the entropy mode does not exist because ρ must follow unperturbed p ; the ρ spectrum would be different especially in a small scale.

We carry out the simulation of isothermal gas with the initial white noise fluctuation. Figure 5 compares the density power spectra adopting the initial white noise perturbations for $\gamma = 1$ (isothermal) and 1.1 at $t = 3$. This figure shows that the density spectrum, which is due to the slow-mode in the isothermal gas, becomes steep nearly $\propto k^{-2}$. Therefore, the imprint of the initial spectrum is unique in the density perturbations of non-isothermal gas, in which entropy-mode perturbation does exist. We should note, however, that the fast-mode turbulence is not influenced whether we adopt isothermal or nonisothermal conditions.

The above result shows that density perturbation in a small scale is influenced by an equation of state of gas. In general, a ratio of specific heat, γ , is controlled by physical processes such as radiative cooling and thermal conduction. This shows that we might get some information on gas properties from observations of density turbulence. Density perturbation is also important in parametric instability because it can work as a mirror against Alfvén and magnetosonic waves. Thus, the relation between γ and density turbulence is interesting. However, unlike fast-mode turbulence, 3D treatment is essential to entropy as well as slow modes, since they are passively advected (Lithwick & Goldreich 2001) and behave very differently in 1D and 3D; we pursue this issue in our future project. In this paper we concentrate on the evolution of the fast mode from now.

4. CASCADING OF FAST MODE

We analyze time-evolution of integrated energy density (energy column density), $\int dx(\rho\delta v^2 + \delta B^2)/2$, of the decaying fast modes.

4.1. Dependence on Initial Amplitude

Figure 6 shows dissipation of fast mode energy as a function of time for different initial amplitudes with the same background $(B_x, B_y) = (9, 3)$. The figure indicates that larger amplitude gives faster damping. This is reasonable since the dissipation is owing to nonlinear processes such as shocks and wave-wave interactions. Damping times, which are defined as slopes of the respective lines, become longer at later times as the amplitudes decrease, which is also consistent with the nonlinear dissipation through steepening.

4.2. quasi-Parallel vs. quasi-Perpendicular

Figure 7 compares the energy of the fast modes of quasi-parallel ($B_x = 9, B_y = 3$) and quasi-perpendicular ($B_x = 3, B_y = 9$) cases. The same $dB_y = 4.4$ and $\gamma = 1.1$ are adopted. The figure shows that the dissipation is more effective in the quasi-perpendicular case. This is because the fast mode shows more compressive character as an angle between the propagation and the magnetic field increases and the shock dissipation is enhanced (Suzuki et al. 2006).

4.3. Dependence on Plasma- β

Since our simulations do not assume isothermal gas, the gas is influenced by the heating, and the plasma- β values change with time by the energy transfer from magnetic fields to gas. This effect is more prominent in the adiabatic cases ($\gamma = 5/3$). We have found from

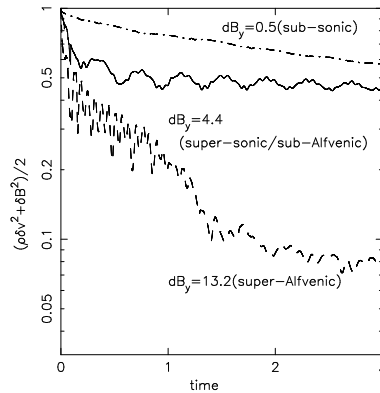


FIG. 6.— Energy of the fast modes of various initial amplitudes. The background field strength is $(B_x, B_y) = (9, 3)$. Dot-dashed, solid, and dashed lines are results of $dB_y = 0.5$ (sub-sonic), 4.4 (super-sonic/sub-Alfvénic), and 13.2 (super-Alfvénic). The initial energy density is normalized at unity in each case.

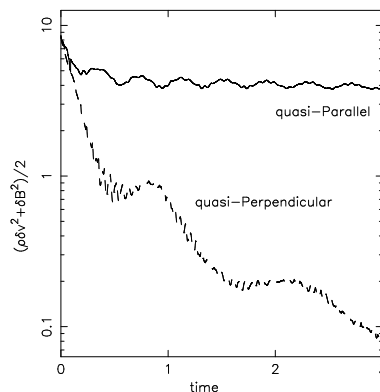


FIG. 7.— Energy (per grid) of the fast modes of the quasi-parallel, $(B_x, B_y) = (9, 3)$, (solid) and quasi-perpendicular, $(B_x, B_y) = (3, 9)$, (dashed) cases.

the simulations that the dependence of the decay of the fast-mode turbulence on plasma- β is very weak provided the plasma is kept magnetically dominated ($\beta < 0.5$) during simulations. However, if β approaches unity, the dissipation becomes saturated.

Figure 8 compares cases with the same $(B_x, B_y) = (9, 3)$ (left) or $(B_x, B_y) = (3, 9)$ (right) and $dB_y = 13.2$ but different $\gamma = 1.1$ (dotted) and $5/3$ (solid). In the case with $\gamma = 5/3$ the plasma is heated up so that the gas pressure eventually becomes comparable with the magnetic pressure ($\beta \simeq 1$). In contrast, the plasma β stays well below unity in the cases with $\gamma = 1.1$ because the heating is less efficient due to the smaller γ . All the three panels of Figure 8 show that once the plasma- β becomes unity the dissipation is suppressed in the case with $\gamma = 5/3$, while the energy density monotonically decreases in the case with $\gamma = 1.1$. In the middle and right panels, the fast-mode energies of the $\gamma = 1.1$ cases are far below those of the $\gamma = 5/3$ cases. Even in the left panel, the energy of the $\gamma = 1.1$ case would be smaller than that of the $\gamma = 5/3$ case, if we proceeded the simulation longer time.

At later epochs in the case with $\gamma = 5/3$, slow mode also has a sizable amount of energy because the phase speed of the slow mode becomes comparable with that of the fast mode. This tendency is more extreme in the quasi-perpendicular case (the right panel), because the

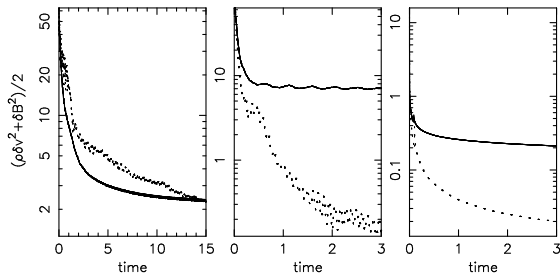


FIG. 8.— *left*: Energy (per grid) of the fast modes of different $\gamma = 1.1$ (dotted) and $5/3$ (solid). The same background field strength, $(B_x, B_y) = (9, 3)$, amplitude, $dB_y = 13.2$, and the initial spectrum, $\propto k^{-3/2}$, are adopted. *middle*: the same as the left panel but for $(B_x, B_y) = (3, 9)$. *right*: the same as the left panel but for the initial white noise spectrum.

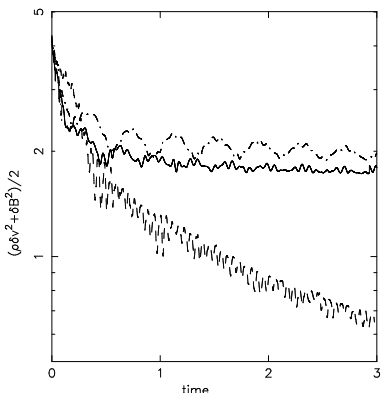


FIG. 9.— Comparison of balanced and imbalanced fast-mode turbulence. Dot-dashed line indicates total fast mode energy in balanced case with $dB_y = 4.4$, solid line indicates fast mode energy propagating to one direction in balanced case with $dB_y = 6.2$, and dashed line denotes fast mode energy in imbalanced case with $dB_y = 4.4$.

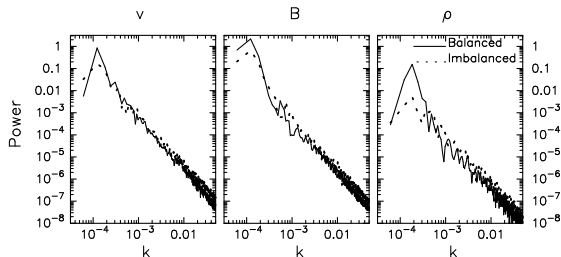


FIG. 10.— Power spectra of the balanced (solid) and imbalanced (dotted) turbulence at $t = 3$.

plasma is heated up more due to larger compressibility.

4.4. *Balanced vs. Imbalanced*

Figure 9 compares the evolution of fast modes in balanced and fully-imbalanced cases. The background field strength is $(B_x, B_y) = (9, 3)$. Dot-dashed line indicates total fast mode energy in balanced case with $dB_y = 4.4$, solid line indicates fast mode energy propagating to one direction in balanced case with $dB_y = 6.2$, and dashed line denotes fast mode energy in imbalanced case with $dB_y = 4.4$. Note that the energy is proportional to dB_y^2 so that the initial values of these three lines are the same. The figure shows that the imbalanced cascade is more dissipative, which is opposed to the tendency obtained in the Alfvénic turbulences.

One reason is different nature of the dissipation of fast and Alfvén modes. The fast mode is isotropic. The dissipation occurs among fast waves which meet the following resonance conditions (see CL02):

$$\omega_1 + \omega_2 = \omega_3, \quad (6)$$

$$\mathbf{k}_1 + \mathbf{k}_2 = \mathbf{k}_3. \quad (7)$$

Since, $\omega \propto k$ for the fast modes, the resonance conditions can be satisfied only when all three \mathbf{k} vectors are collinear. When parent '1' and '2' waves propagate in the counter directions, (different signs of \mathbf{k}_1 and \mathbf{k}_2) the daughter wave should have smaller wavenumber, \mathbf{k}_3 , (larger wavelength).

In contrast, if parent waves propagate in the same direction, wavenumber of the daughter wave becomes larger than the parents', which is more appropriate for the dissipation. In the imbalanced case, we only have fast modes traveling in the same direction so that the resonances selectively generate waves with shorter wavelengths which suffer faster dissipation. Dot-dashed (energy of one direction in balanced case with $dB_y = 6.2$) and dashed (imbalanced case with $dB_y = 4.4$) lines show very similar damping at the beginning ($t \leq 0.5$). This indicates that the dissipation of 1D fast mode turbulence is controlled by wave packets traveling in the same direction and almost independent of those in the counter directions during this period, since the initial energy of one direction in the former case is identical to the initial total energy of the latter.

In later time, however, the dissipation of the balanced cases is slower than the dissipation of the imbalanced case. To investigate this difference, we compare the power spectra at $t = 3$ (Figure 10). The comparison shows that more power is kept at very small $k \approx 10^{-4}$ in the balanced turbulence, although both show the shock-dominated spectra, $\propto k^{-2}$, in the higher k regime. This might indicate that a kind of inverse cascade takes place preferentially in the balanced turbulence. Since turbulences with larger scales (smaller k) suffer less damping, further dissipation seems suppressed in the balanced turbulence. However, we think that to discuss this issue the 1D simulation is not sufficient, hence, we leave it to our future studies.

We also suspect that bulk acceleration affects the faster dissipation of the imbalanced fast-mode turbulence. The imbalanced flux of fast mode transfers the momentum flux to the fluid. As a result, the system is accelerated into the direction corresponding to the initial wave momentum flux. Generally, energy density of waves is lost in accelerating fluid by transfer of the momentum flux to the gas even though the waves themselves do not suffer damping (Jacques 1977). However, after comparison of the bulk momentum flux of the gas with the dissipated energy of the fast-mode turbulence, we have found that the effect of the bulk acceleration is not so large ($< 10\%$) in our case.

5. SUMMARY AND DISCUSSIONS

We have shown that the imbalanced fast modes dissipate in a different way than Alfvén ones. For the Alfvén turbulence cascading is due to wave packets moving in the opposite direction, therefore, the imbalance makes the cascading less efficient. For fast modes waves

moving in the same direction interact more efficiently. We confirmed that the oppositely moving fast modes are not essential for the cascading as discussed earlier (see CL02).

However, the obtained power spectrum (k^{-2}) is different from the weak acoustic turbulence ($k^{-3/2}$) suggested in CL02, which may be owing to the different geometries (1D vs. 3D) as discussed in §3. We should note that this problem of the scaling of acoustic turbulence is not settled down because the approximation of weak cascade is controversial (Falkovich & Meyer 1996; Zakharov, L'vov, & Falkovich 1992). It is clear that further research by 3D simulations with a sufficient inertial range is necessary.

We have also found that as the amplitude of compressions increase, the non-linear damping of turbulence speeds up. In our adiabatic calculations the restoring force was increasing due to medium heating and as the result the non-linear steepening and cascading slowed down. Similarly, for the modes that compress both magnetic field and gas, the rate of dissipation was less compared to the modes that mostly compress the gas.

The density perturbation is mainly carried by slow mode perturbation in the large scale and entropy mode in the small scale perturbation in non-isothermal gas. The slow-mode density spectrum is dominated by shocks, $\propto k^{-2}$, while the entropy-mode, which is a consequence of the dissipation of the initial fast-mode turbulence, preserves the initial turbulent spectrum. As a result, the spectral index of the density perturbation is subject to the initial spectrum of given fast-mode turbulence. In isothermal gas, density spectrum is different in a small scale because entropy-mode fluctuation does not exist. This shows that to study density turbulence one has to carefully treat driving properties of turbulence and to take into account appropriate thermal processes (e.g. Koyama & Iutsuka 2002; Larson 2005) rather than assume a polytropic equation of state. While the density turbulence is an interesting issue, obviously 3D treatment is required since the slow- and entropy-mode perturbation is different in 1D and 3D circumstances; we will study this topic in a future paper.

In this paper we have focused on the fast-mode in low- β medium. Various interstellar/intergalactic medium is dominated by magnetic pressure rather than gas pressure, i.e., low- β condition. Referring to the tabulation in YL04 (Table 1 in their paper), galactic halo, and warm and cold ISM are mildly low- β ($\beta = 0.1 - 1$), and dark clouds are more magnetically dominated, $\beta = 0.01 - 0.1$. Our simulations are directly applicable to these media.

Magnetospheres of general stars with surface convection (like the sun) and compact objects (white dwarfs and neutron stars) are also in low- β condition, because the density rapidly decreases upwards. Moreover, the turbulence tends to be imbalanced there because it is mainly generated from central stars and dominated by the outward component. Our results show that the fast mode is likely to be the culprit in the heating and acceleration of winds because it dissipates effectively even without the inward component. The advantage of the fast-mode versus Alfvénic turbulence in the stellar wind acceleration is that the latter requires production of counter-waves via reflection or by some other mechanism.

Cascading of imbalanced fast modes is important for the problem of streaming instability evolution, which is the part of the picture of both galactic leaky box model and the acceleration of particles in shocks. This instability arises from the flow of particles along the magnetic field direction and reflects the particles back (Kulsrud & Pearce 1968). Our results indicate that the fast mode cascading limits the instability even in the absence of both damping and the ambient turbulence (YL02, Farmer & Goldreich 2004).

In our simulation the dissipation is mainly due to MHD shocks besides sub-grid scale damping. However, if we discuss the dissipation in more detail, we need to take into account the microphysics. Galactic halo and stellar winds generally consist of collisionless plasma. In such conditions, the fast-mode as well as slow-mode fluctuations possibly dissipate by transit-time damping (e.g. Barnes 1966; Suzuki et al. 2006). In warm ionized ISM, the dissipation is mainly due to Coulomb collisions. If there is a considerable fraction of neutral atoms, e.g. in cold ISM and dark clouds, collisions between neutrals and ions dominate (see Table 1 in YL04).

Turbulence may be very different in 1D and 3D. We find, however, that our attempts to get insight into the dynamics of fast modes using 1D model is meaningful, as the possible transversal deviation δk is limited. Assuming that the fast modes follow the acoustic cascade with the cascading time

$$\tau_k = \omega/k^2 v_k^2 = (k/L)^{-1/2} \times V_{ph}/V^2, \quad (8)$$

YL04 used the uncertainty condition $\delta\omega t_{cas} \sim 1$, where $\delta\omega \sim V_{ph}\delta k(\delta k/k)$ to estimate δk

$$\delta k/k \simeq \frac{1}{(kL)^{1/4}} \left(\frac{V}{V_{ph}} \right)^{1/2}. \quad (9)$$

Eq. (9) provides a very rough estimate of how much the randomization of vectors is expected due to the fast mode cascading. This estimates suggest that deep down the cascade where $kL \gg 1$ the approximation of waves moving in the same direction could be accurate enough.

In this paper we dealt with fast modes irrespectively of the evolution of the other modes. This possibility corresponds to the earlier theoretical and numerical studies (GS95, Lithwick & Goldreich 2001, CL02, CL03). Recently, however, Chandran (2005) discussed the interaction between fast and Alfvén modes under the approximation that the latter constitute *weak* turbulence, i.e. turbulence that cascades slowly due to weak non-linearities. We expect appreciable mitigation of the Alfvén-fast mode interaction compared to those in Chandran (2005), when Alfvénic turbulence is *strong*, i.e. when the turbulence evolves fast, over just one wave period. We feel that the resulting large disparity in the rate of evolution of the Alfvénic and fast modes should result in much less cascading of fast modes by the Alfvénic modes compared to the case of the weak Alfvénic turbulence. Note, that strong Alfvénic turbulence is default for most astrophysical situations, while the inertial range of the weak Alfvénic turbulence is limited⁵ (Goldreich &

⁵ It is easy to see that if the injection happens at scale L with Alfvén Mach number $M_A = V/V_A$, where V_A is the Alfvén velocity that arises from the total magnetic field in the fluid, the range for

Sridhar 1997, Lazarian & Vishniac 1999). In our next paper we shall provide calculations of the fast modes interaction with the Alfvénic modes.

Acknowledgments

T.K.S. is supported by JSPS Research Fellow for Young Scientist, 4607, and a Grant-in-Aid for Scien-

tific Research, 18840009, from MEXT of Japan. AL acknowledges the support of the NSF Center for Magnetic Self-Organization in Laboratory and Astrophysical Plasmas and the NSF grant AST-0307869 and NSF-ATM-0312282. AB acknowledges the support of the Ice Cube project.

weak turbulence is limited by $[L, LM_A^2]$. While the regime of weak Alfvénic turbulence can still be important (see Lazarian 2006), in most astrophysical situations that regime of strong Alfvénic turbulence covers much longer inertial range.

REFERENCES

- Alfvén, H. & Fälthammar, C.-G. 1964, *Zeitschrift für Astrophysik*, 58, 292
- Ballesteros-Paredes, J., Klessen, R. S., MacLow M.-M., & Vázquez-Semadeni, E. 2006, *Proto-Stars & Planets V*, pre-print (astro-ph/0603357)
- Barnes, A. 1966, *Phys. Fluid*, 9, 1483
- Beresnyak, A., Lazarian, A., Cho, J. 2005, *ApJ*, 624, L93
- Chandran, B. D. G. 2000, *Phys. Rev. Lett.*, 85, 4656
- Chandran, B. D. G. 2005, *Phys. Rev. Lett.*, 95, 5004
- Cho, J., Lazarian, A., & Vishniac, E. T. 2003, *Turbulence and magnetic fields in astrophysics*, eds. T. Passot & E. Falgarone, LNP 614, Springer, Berlin, astro-ph/0205286
- Cho, J. & Lazarian, A. (2002), *Phys. Rev. Lett.*, 88, 245001
- Cho, J. & Lazarian, A. (2003), *MNRAS*, 345, 325 - 339
- Elmegreen, B. C. & Falgarone, E. 1996, *ApJ*, 471, 816
- Elmegreen, B. C. 2002, *ApJ*, 577, 206
- Falkovich, G. & Meyer, M. 1996, *Phys. Rev. E*, 54, 4431
- Farmer, A. J. & Goldreich, P. 2004, 604, 671
- Goldreich, P. & Sridhar, S. 1995, *ApJ*, 438, 763
- Goldreich, P. & Sridhar, S. 1997, *ApJ*, 485, 680
- Higdon, J. C. 1984, *ApJ*, 285, 109
- Jacques, S. A. 1977, *ApJ*, 215, 942
- Kim, J. & Ryu, D. 2005, *ApJ*, 630, L45
- Koyama, H. & Inutsuka, S. 2002, *ApJ*, 564, L97
- Kulsrud & Pearce 1968
- Larson, R. B. 2005, *MNRAS*, 359, 211
- Lazarian, A. 2006, *ApJL*, 645, L25
- Lazarian, A. & Vishniac, E. 1999, *ApJ*, 517, 700
- Lazarian, A. & Yan, H. 2002, *ApJ*, 556, L105
- Lithwick, Y. & Goldreich, P. 2001, *ApJ*, 562, 279
- Lyubarsky, Y. E. 2003, *MNRAS*, 339, 765
- McKee, C. F. & Tan, J. C. 2002, *Nature*, 6876, 59
- Montgomery, D., Brawn, M. R., & Matthaeus, W. H. 1987, *J. Geophys. Res.*, 92, 282
- Passot T. & Vázquez-Semadeni, E. 2003, *A&A*, 398, 845
- Pudritz, R. E. 2002, *Science*, 295, 68
- Shebalin, J. V., Matthaeus, W. H., & Montgomery, D. 1983, *J. Plasma Phys.*, 29, 525
- Shebalin, J. V. & Montgomery, D. 1988, *J. Plasma, Phys.*, 39, 339
- Stutzki, J. 2001, *Ap&SSSupp.*, 277, 39
- Suzuki, T. K., Yan, H., Lazarian, A., Cassinelli, J. P. 2006, *ApJ*, in press
- Suzuki, T. K. & Inutsuka, S. 2005, *ApJ*, 632, L49
- Suzuki, T. K. & Inutsuka, S. 2006, *J. Geophys. Res.*, in press
- Tsuji, T. 1988, *A&A*, 197, 185
- Tu, C.-Y. & Marsch, E. 1995, *Space Sci. Rev.*, 73, 1
- Yan, H. & Lazarian, A. 2002, *Phys. Rev. Lett.*, 89, 1102
- Yan, H. & Lazarian, A. 2003, *ApJ*, 592, L33
- Yan, H. & Lazarian, A. 2004, *ApJ*, 614, 757
- Zakharov, V. E., L'vov, V. S., & Falkovich, G. 1992, *Kolmogorov Spectra of Turbulence I*, *Springer-Verlag*
- Zank, G. P. & Matthaeus, W. H. 1992, *J. Geophys. Res.*, 97, 17189